

# Multicue MRF Image Segmentation: Combining Texture and Color Features\*

Zoltan Kato<sup>†</sup>, Ting-Chuen Pong\*, Song Guo Qiang

National University of Singapore, School of Computing, 3 Science Drive 2, Singapore 117543, Fax: +65 779 4580,

\* Hong Kong University of Science & Technology, Computer Science Dept., Clear Water Bay, Hong Kong, Fax: +852 2358 1477,

E-mail: kato@inf.u-szeged.hu, tcpong@cs.ust.hk, songguoq@comp.nus.edu.sg

## Abstract

Herein, we propose a new Markov random field (MRF) image segmentation model which aims at combining color and texture features. The model has a multi-layer structure: Each feature has its own layer, called feature layer, where an MRF model is defined using only the corresponding feature. A special layer is assigned to the combined MRF model. This layer interacts with each feature layer and provides the segmentation based on the combination of different features. The uniqueness of our algorithm is that it provides both color only and texture only segmentations as well as a segmentation based on combined color and texture features. The number of classes on feature layers is given by the user but it is estimated on the combined layer.

## 1. Introduction

Image segmentation is an important early vision task where pixels with similar features are grouped into homogeneous regions. There are many features that one can take into account during the segmentation process: gray-level, color, motion, texture features, etc. However, most of the segmentation algorithms presented in the literature are based on only one of the above features. Recently, the segmentation of color images received more attention [2, 5, 10, 9, 11, 8]. In this paper, we are interested in the segmentation of color textured images. Basically, there are two approaches to this problem: One approach deals directly with *color textures* [10, 9]. In [10], an unsupervised segmentation algorithm is proposed which uses Gaussian MRF models for *color textures*. These models are defined in each color plane with interactions between different color planes. The segmentation algorithm is based on agglomerative hierarchical clustering. A different approach is presented in [9] which uses a multiband smooth-

ing algorithm to generate a multiscale representation of an image. The smoothing is based on human psychophysical measurements of color appearance. First the coarsest level is clustered to isolate core clusters. Other pixels are then reassigned to these core clusters using a probabilistic assignment. Another frequently used approach tries to combine traditional gray level texture features together with pure color features [11, 8]. Our approach falls into this category.

The novelty of our model can be summarized as follows: First, we use *different* features at different layers. This allows us to work with different models or to have varying number of regions at different layers, choosing the one which describes the best our feature data at a given layer. In addition, we have a special layer, called *combined layer*, which does not correspond to any feature but provides a way to combine different features. Second, the layers are fully connected: each pixel interacts with the corresponding pixel at other layers. A similar, fully connected pyramidal model is used in [7]. Multiscale pyramids have also been successfully applied for image segmentation [4]. In these models, each layer usually contains the *same* image data at different resolutions. However, we use *different* data at different layers and we do not perform subsampling, therefore our model is not a pyramid. Each layer is of the same size. In this respect, our model is similar to [10, 9].

## 2. Multi-Layer Segmentation Model

We use perceptually uniform CIE-L\*u\*v\* color values and texture features derived from the Gabor filtered gray-level image. Segmentation requires simultaneous measurements in both spatial and frequency domain. However, spatial localization of boundaries requires larger bandwidths whereas smaller bandwidths give better texture measurements. Fortunately, Gabor filters have optimal joint localization in both domains [6]. In addition, when we are combining texture features with color, the spatial resolution is considerably increased.

Our model consists of 3 layers. At each layer, we use

\*partially supported by grant HKUST6072/97E

<sup>†</sup>Currently with the Dept. of Informatics, University of Szeged, Hungary

a first order neighborhood system and higher order inter-layer cliques (Fig. 1). The image features are represented by multi-variate Gaussian distributions. Herein, we do not address parameter estimation but we note that the task can be solved using an adaptive segmentation technique [12].

Let us denote the color layer by  $\mathcal{S}^c$ , the texture layer by  $\mathcal{S}^t$  and the combined layer by  $\mathcal{S}^x$ . All layers are of the same size. Our MRF model is defined over the lattice  $\mathcal{S} = \mathcal{S}^c \cup \mathcal{S}^x \cup \mathcal{S}^t$ . For each site  $s$ , the region-type (or class) that the site belongs to is specified by a class label,  $\omega_s$ , which is modeled as a discrete random variable taking values in  $\Lambda = \{1, 2, \dots, L\}$ . The set of these labels  $\omega = \{\omega_s, s \in \mathcal{S}\}$  is a random field, called the *label process*. Furthermore, the observed image features (color and texture) are supposed to be a realization  $\mathcal{F} = \{\mathbf{f}_s | s \in \mathcal{S}^c \cup \mathcal{S}^t\}$  from another random field, which is a function of the label process  $\omega$ . Basically, the *image process*  $\mathcal{F}$  represents the deviation from the underlying label process. Thus, the overall segmentation model is composed of the hidden label process  $\omega$  and the observable noisy image process  $\mathcal{F}$ . Our goal is to find an optimal labeling  $\hat{\omega}$  which maximizes the a posteriori probability  $P(\omega | \mathcal{F})$ , that is the *maximum a posteriori* (MAP) estimate [3]:  $\arg \max_{\omega \in \Omega} P(\omega | \mathcal{F}) = \arg \max_{\omega \in \Omega} \prod_{s \in \mathcal{S}} P(\mathbf{f}_s | \omega_s) P(\omega)$ , where  $\Omega$  denotes the set of all possible labelings. We use the ICM algorithm [1] to obtain a suboptimal MAP estimate. According to the *Hammersley-Clifford theorem* [3],  $P(\omega | \mathcal{F})$  follows a Gibbs distribution:

$$P(\omega | \mathcal{F}) = \frac{\exp(-U(\omega))}{Z(\beta)} = \frac{\prod_{C \in \mathcal{C}} \exp(-V_C(\omega_C))}{Z(\beta)} \quad (1)$$

where  $U(\omega)$  is called an *energy function*,  $Z(\beta) = \sum_{\omega \in \Omega} \exp(-U(\omega))$  is the normalizing constant and  $V_C$  denotes the *clique potential* of clique  $C \in \mathcal{C}$  having the label configuration  $\omega_C$ . Note that the energies of *singletons* (ie. cliques of single sites  $s \in \mathcal{S}$ ) directly reflect the probabilistic modeling of labels without context, while higher order clique potentials express relationship between neighboring pixel labels. In the remaining part of this section, we will define these clique potentials for each layer.

## 2.1. Color Layer

On the color layer, the observed image  $\mathcal{F}^c = \{\mathbf{f}_s^c | s \in \mathcal{S}^c\}$  consists of three spectral component values ( $\mathbf{L}^* \mathbf{u}^* \mathbf{v}^{*}$ ) at each pixel  $s$  denoted by the vector  $\mathbf{f}_s^c$ . We assume that  $P(\mathbf{f}_s^c | \omega_s)$  follows a Gaussian distribution, the classes  $\lambda \in \Lambda^c = \{1, 2, \dots, L^c\}$  are represented by the mean vectors  $\bar{\mu}_{\lambda}^c$  and the covariance matrices  $\Sigma_{\lambda}^c$ . The class label assigned to a site  $s$  on the color layer is denoted by  $\psi_s$ . The energy function  $U(\psi, \mathcal{F}^c)$  of the so defined MRF layer has

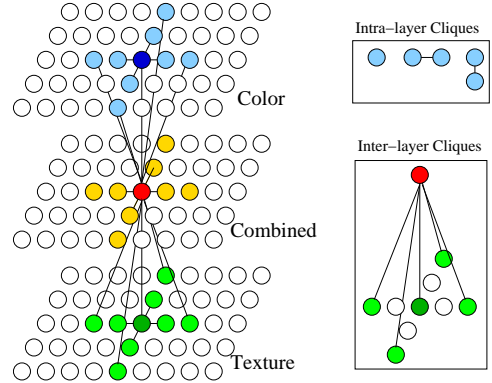


Figure 1. Multi-layer MRF model.

the following form:

$$\sum_{s \in \mathcal{S}^c} \mathcal{G}^c(\mathbf{f}_s^c, \psi_s) + \beta \sum_{\{s, r\} \in \mathcal{C}} \delta(\psi_s, \psi_r) + \gamma^c \sum_{s \in \mathcal{S}^c} V^c(\psi_s, \eta_s^c)$$

Since we assume that  $P(\mathbf{f}_s^c | \omega_s)$  is Gaussian, it follows from Eq. (1) that the corresponding energy potentials  $\mathcal{G}^c(\mathbf{f}_s^c, \psi_s)$  should be log Gaussians:

$$\ln(\sqrt{(2\pi)^3 |\Sigma_{\psi_s}^c|}) + \frac{1}{2}(\mathbf{f}_s^c - \bar{\mu}_{\psi_s}^c) \Sigma_{\psi_s}^{c-1} (\mathbf{f}_s^c - \bar{\mu}_{\psi_s}^c)^T \quad (2)$$

$\delta(\psi_s, \psi_r) = 1$  if  $\psi_s$  and  $\psi_r$  are different and  $-1$  otherwise.  $\beta > 0$  is a parameter controlling the homogeneity of the regions. As  $\beta$  increases, the resulting regions become more homogeneous. The last term ( $V^c(\psi_s, \eta_s^c)$ ) is the inter-layer clique potential which will be defined later and  $\gamma^c$  is a parameter controlling the influence of the combined layer. As  $\gamma^c$  increases, the influence is higher.

## 2.2. Texture Layer

On the texture layer, the observation consists of a set of Gabor image features. To obtain these features, we use the multi-channel filtering approach [6]: The channels are represented by a bank of real-valued, even-symmetric Gabor filters. In our tests, we used four orientations:  $0^\circ, 45^\circ, 90^\circ, 135^\circ$  and the radial frequencies  $u_0$  were 1 octave apart:  $\sqrt{2}, \sqrt{2}/2, \sqrt{2}/4, \sqrt{2}/8, \dots$ . We automatically select 6 of these filtered images such that they cover more than 99% of the image's intensity variations (see [6] for more details). From each filtered image  $g$ , we compute a *feature image* using the nonlinear transformation  $|\tanh(\alpha g_s)|$ ,  $s \in \mathcal{S}^t$  followed by a Gaussian blurring with a deviation proportional to the center frequency of the Gabor filter:  $\sigma = k/u_0$ . In our experiments, the Gabor filtered images are scaled to the interval  $[-1, 1]$  and we set  $\alpha = 40$  and  $k = 1$ .

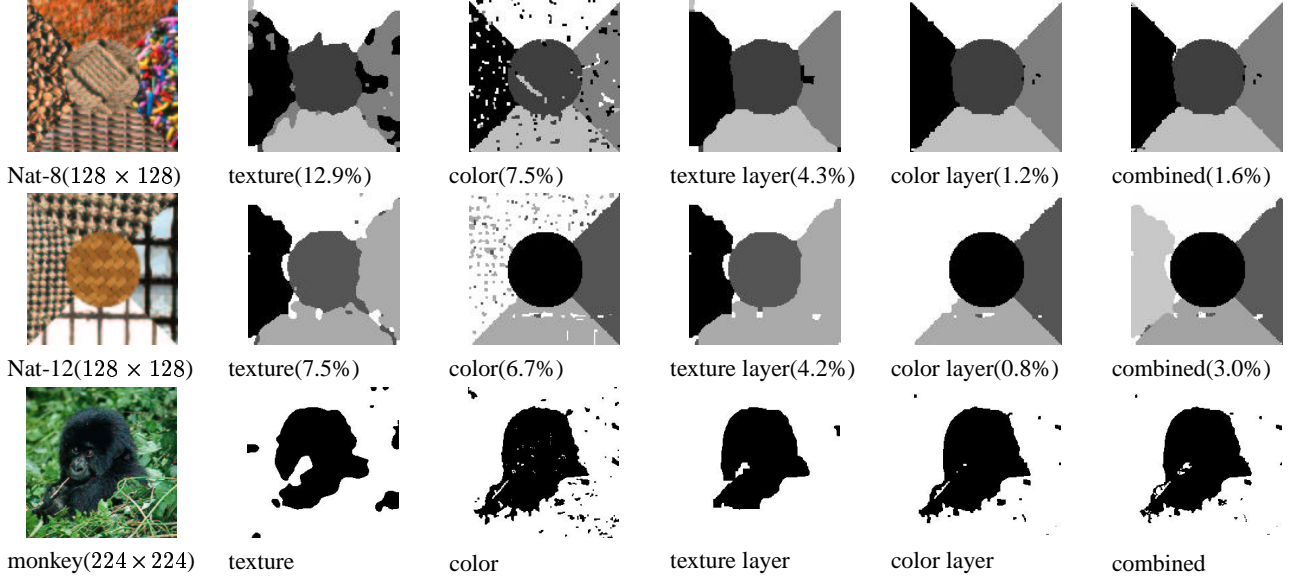


**Figure 2.** Results and misclassification rate of color only, texture only, and combined models

The MRF model itself is quite similar to the one outlined in the previous section. The only difference is that the observation consists of 6 dimensional texture feature vectors  $\mathcal{F}^t = \{\vec{f}_s^t | s \in \mathcal{S}^t\}$ . The energy of higher order cliques is  $\xi \sum_{\{s,r\} \in \mathcal{C}} \delta(\phi_s, \phi_r) + \gamma^t \sum_{s \in \mathcal{S}^t} V^t(\phi_s, \eta_s^t)$ , where  $\xi$  (resp.  $\gamma^t$ ) has the same role as  $\beta$  (resp.  $\gamma^c$ ) in the color layer. Furthermore,  $\phi_s$  denotes the label assigned to a site  $s$ . As in the previous case, classes are represented by the mean vectors  $\mu_{\vec{\lambda}}^t$  and the covariance matrices  $\Sigma_{\vec{\lambda}}^t$ . The inter-layer clique potential ( $V^t(\phi_s, \eta_s^t)$ ) will be defined later.

### 2.3. Combined Layer

The combined layer only uses the texture and color features indirectly, through inter-layer cliques. A label consists of a pair of color and texture labels such that  $\eta = \langle \eta^c, \eta^t \rangle$ , where  $\eta^c \in \Lambda^c$  and  $\eta^t \in \Lambda^t$ . The set of labels is denoted by  $\Lambda^x = \Lambda^c \times \Lambda^t$  and the number of classes  $L^x = L^c L^t$ . Obviously, not all of these labels are valid for a given image. Therefore the combined layer model also estimates the number of classes and chose those pairs of texture and color labels which are actually present in a given image. The energy function  $U(\eta) = \sum_{s \in \mathcal{S}^x} (V_s(\eta_s) + \rho^c V^c(\psi_s, \eta_s^c) + \rho^t V^t(\phi_s, \eta_s^t)) + \alpha \sum_{\{s,r\} \in \mathcal{C}} \delta(\eta_s, \eta_r)$  where  $V_s(\eta_s)$  denotes singleton energies,  $V^c(\psi_s, \eta_s^c)$  (resp.  $V^t(\phi_s, \eta_s^t)$ ) denotes inter-layer clique potentials. The last term corresponds to second order intra-layer cliques which ensures homogeneity of the combined layer.  $\alpha$  has the same role as  $\beta$  in the color layer model and  $\delta(\eta_s, \eta_r) = -1$  if  $\eta_s = \eta_r$ , 0 if  $\eta_s \neq \eta_r$  and 1 if

$\eta_s^c = \eta_r^c$  and  $\eta_s^t \neq \eta_r^t$  or  $\eta_s^c \neq \eta_r^c$  and  $\eta_s^t = \eta_r^t$ . The idea is that region boundaries present at both color and texture layers are preferred over edges that are found only at one of the feature layers. Inter-layer interactions are as follows:

$$V^c(\psi_s, \eta_s^c) = \sum_{\{s,r\} \in \mathcal{C}_6} W_r D^c(\psi_r, \eta_s^c)$$

where  $D^c(\psi_r, \eta_s^c) = | \mathcal{G}^c(\vec{f}_r^c, \psi_r) - \mathcal{G}^c(\vec{f}_s^c, \eta_s^c) |$  (see Eq. (2)).  $V^t(\phi_r, \eta_s^t)$  and  $D^t(\phi_r, \eta_s^t)$  are defined in a similar way using texture features. At any site  $s$ , we have a clique between two layers containing 6 sites (the set of these inter-layer cliques is denoted by  $\mathcal{C}_6$ ), which implements 5 inter-layer interactions: Site  $s$  interacts with the corresponding site on the other layer as well as with the 4 neighboring sites two steps away (see Fig. 1).  $W_r$  is the weight of the clique  $\{s, r\} \in \mathcal{C}_6$ . We assign higher weight (0.6) to the corresponding site whereas smaller weights (0.1 each) to the other 4 neighboring sites. The latter 4 sites help to ensure homogeneity on the combined layer. Note that  $D^c$  and  $D^t$  corresponds to the difference of the first order potentials at the corresponding feature layer. Clearly, the difference is 0 if and only if both the feature layer and the combined layer has the same label. If the labels are different then it is proportional to the energy difference between the two labels.  $\rho^c$  (resp.  $\rho^t$ ) controls the influence of the inter-layer cliques on the combined layer. A higher value will increase the importance of the information coming from the corresponding feature layer. Note that we have a similar weight ( $\gamma^c, \gamma^t$ ) at the feature layers. The difference of these weights balances the influence of the feature layers to the combined layer vs.

combined layer to the feature layers. Therefore, depending on the value of  $\rho^t$  (resp.  $\rho^c$ ), we can increase ( $\gamma > \rho$ ) or decrease ( $\gamma < \rho$ ) the influence of a feature layer to the combined layer without changing the influence of the combined layer to a feature layer. We found this an important issue in the case of the texture layer.

The singleton energy is defined as  $V_s(\eta_s) = R((10N_{\eta_s})^{-3} + \mathcal{P}(L))$ . It controls the number of classes at the combined layer.  $(10N_{\eta_s})^{-3}$  penalizes small classes ( $N_{\eta_s}$  is the percentage of the sites assigned to class  $\eta_s$ ), while  $\mathcal{P}(L)$  includes some prior knowledge about the number of classes. Currently this is expressed by a log Gaussian term (similar to the one in Eq. (2)) with mean value  $\hat{L}$  (basically an initial guess) and variance  $\sigma$  (confidence in the initial guess).  $R$  is simply a weight of this term, we set it to 0.5 in our tests.

### 3. Experiments

The proposed algorithm has been tested on a variety of synthetic and real images. The computing time was 2-4 minutes on a Pentium III 933. We also compare the results to texture only and color only segmentation (basically a monogrid model similar to the one defined for the feature layers but without inter-layer cliques). The mean vectors and covariance matrices were computed over representative regions selected by the user. The number of texture and color classes is known a priori but classes on the combined layer are estimated during the segmentation process. Hyperparameters have been trained on a small subset of images:  $\alpha = 1.0$ ,  $\beta = \xi = 10.0$ ,  $\gamma^c = \gamma^t = 1.5$ ,  $\rho^c = 0.5$ , and  $\rho^t = -0.3$ . These values have been found to provide satisfactory results on *all* test images. The values of  $\beta$  and  $\xi$  are not crucial, basically any value between 2 and 15 provides good segmentations.  $\gamma$  and  $\rho$  values need slightly higher accuracy. Note that by setting  $\rho^t < 0$  and  $\rho^c > 0$ , we decrease the influence of the texture layer and increase the influence of the color layer on the combined layer. This is necessary because texture features (due to filtering and blurring) have weaker spatial localization. Hence, we give a higher weight to the color layer so that edges will be localized correctly while region homogeneity (where color layer is slightly weaker, especially in textured regions) is still maintained. Fig. 2 shows some segmentation results together with the measured misclassification rate. Clearly, the multi-layer model provides significantly better results compared to color only and texture only segmentations. *Nat-12* shows an image with 4 different textures and 4 different colors. We can see, that our method provides accurate segmentations on both feature layers and it is also able to detect 5 classes on the combined layer. Note that the combined layer produces slightly higher misclassification rates ( $\approx 0.5\%$ ) than the color layer. This is due to sharper boundaries on the

color layer (texture has weaker spatial resolution and the combined layer is directly influenced by the texture layer). We have also compared our results to those reported in [9] and found them equally good. One example is the *monkey* image but more results are available on our website ([www.cs.ust.hk/~kato/research/icpr2002/](http://www.cs.ust.hk/~kato/research/icpr2002/)).

### 4. Conclusion

We have proposed a new multi-layer MRF segmentation model which successfully combines color and texture features. However, the model is not restricted to these features. It can be applied to multicue segmentation in general. Although the current implementation doesn't estimate model parameters (except number of classes on the combined layer), it is possible to use an adaptive segmentation technique [12] to tackle this problem. This issue is currently under investigation.

### References

- [1] J. Besag. On the statistical analysis of dirty pictures. *J. Roy. Statist. Soc., ser. B*, 1986.
- [2] D. Comaniciu and P. Meer. Robust analysis of feature spaces: Color image segmentation. In *Proc. of CVPR*, pages 750–755, San Juan, Puerto Rico, June 1997.
- [3] S. Geman and D. Geman. Stochastic relaxation, Gibbs distributions and the Bayesian restoration of images. *IEEE Trans. on PAMI*, 6:721–741, 1984.
- [4] F. Heitz, P. Perez, and P. Boutheymy. Multiscale Minimization of Global Energy Functions in Some Visual Recovery Problems. *CVGIP:JU*, 59(1):125–134, 1994.
- [5] C. L. Huang, T. Y. Cheng, and C. C. Chen. Color images segmentation using scale space filter and Markov random field. *Pattern Recognition*, 25(10):1217–1229, 1992.
- [6] A. K. Jain and F. Farrokhnia. Unsupervised texture segmentation using Gabor filters. *Pattern Recognition*, 24(12):1167–1186, 1991.
- [7] Z. Kato, M. Berthod, and J. Zerubia. A hierarchical Markov random field model and multi-temperature annealing for parallel image classification. *CVGIP: GMIP*, 58(1):18–37, Jan. 1996.
- [8] W. Y. Ma and B. S. Manjunath. Edge flow: A framework of boundary detection and image segmentation. In *Proc. of CVPR*, pages 744–749, San Juan, Puerto Rico, June 1997.
- [9] M. Mirmehdi and M. Petrou. Segmentation of color textures. *IEEE Trans. PAMI*, 22(2):142–159, Feb. 2000.
- [10] D. K. Panjwani and G. Healey. Markov random field models for unsupervised segmentation of textured color images. *IEEE Trans. PAMI*, 17(10):939–954, Oct. 1995.
- [11] S. C. Tan and J. Kittler. Colour texture classification using features from color histogram. In *Proc. 8<sup>th</sup> SCIP*, 1993.
- [12] C. S. Won and H. Derin. Unsupervised segmentation of noisy and textured images using Markov random fields. *CVGIP: GMIP*, 54(4):208–328, July 1992.